Particle tracing and acceleration in MHD evolution

Oliver Porth
with some material from Bart Ripperda

September 15, 2015

Overview

Motivation

Applications
- Examples from recent literature
- Particle transport in Pulsar Wind Nebulae: MPI-AMRVAC simulations

Guiding Centre Approximation

The examples of the Hands-On-Session

- Fluid models: Good for global dynamics and energetics
- Fail to tell you anything about kinetic processes
- Kinetic models: The opposite...

- Assume fluid models are largely correct and see how particles with given energies would behave in the overall flow.
- Use for further diagnostic, see applications...

Trapping of solar wind particles in earth magnetosphere

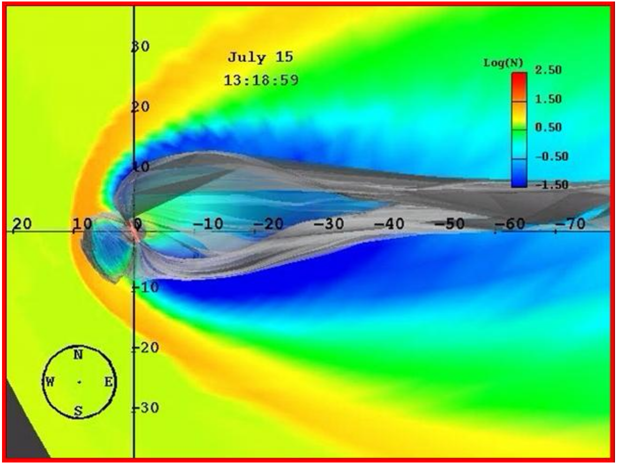

Figure : LFM model of the earth magnetosphere, Credit: CISM

Trapping of solar wind particles in earth magnetosphere

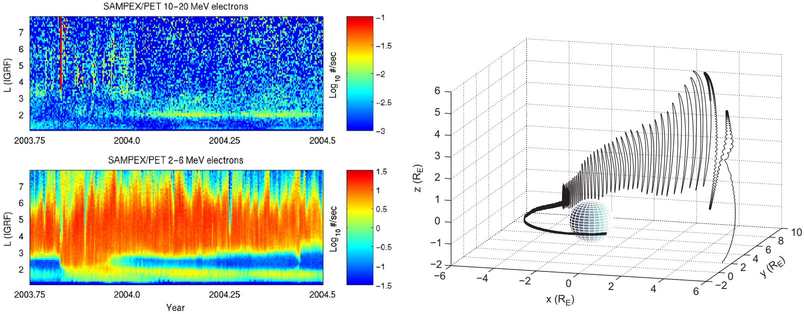

Figure : SSE captured in magnetosphere in "Halloween storm"

Solar electrons and outer belt electrons establish a new $> 10\mathrm{MeV}$ radiation belt. Kress et al. (2007) Kress et al. (2008)

Trapping of solar wind particles in earth magnetosphere

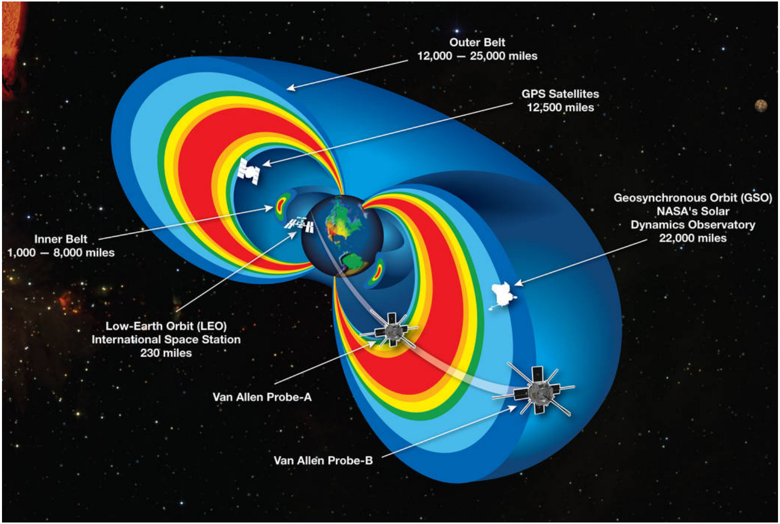

Figure : Earth radiation belts

Trapping of solar wind particles in earth magnetosphere

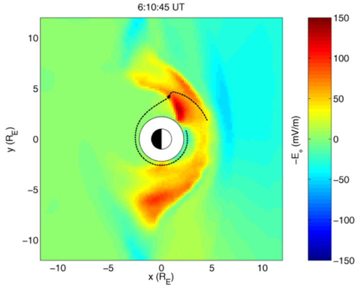

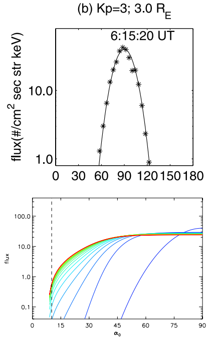

During solar storm, outer belt electrons (adiabatically) accelerated in storm $E_\phi \Rightarrow$

- Peaked pitchangle distribution.
- Formation of new belt related to slow pitch-angle diffusion $\sim$ several months.

Transport modelling

Particle transport in diffusion limit described via Fokker-Planck type transport equation

$$\frac{\partial f}{\partial t} + \mathbf{v} \cdot \nabla f = \frac{\partial}{\partial \mu}\left(D_{\mu\mu}\frac{\partial f}{\partial \mu}\right) + \frac{1}{p^2}\frac{\partial}{\partial p}\left(D_{pp}\frac{\partial f}{\partial p}\right) \tag{1}$$

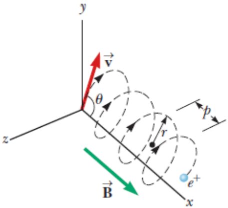

with Pitch angle dependence $\mu = \cos\alpha$.

Quasi linear theory (QLT) provides diffusion coefficients $D_{\mu\mu}$, D_{pp} in terms of the (turbulent) spectrum of magnetic fluctuations (e.g. Jokipii, 1966).

Particle transport and acceleration in (turbulent) plasma key process in high energy astrophysics!

QLT and its problems

- Given the spectrum of magnetic anomalies, $P(k) \propto k^{-q}$
- Assume guiding-centres are unperturbed
- Assume only resonant $|s| = 1$ wave-particle interactions
- Assume small amplitude broadband and incoherent waves (stochastic)

$$D_{\mu\mu} = \frac{\nu(\mu)}{2}(1-\mu^2) \qquad (2)$$

$$\lambda_{||} = \frac{3v}{8}\int_{-1}^{1} d\mu \frac{(1-\mu^2)^2}{D_{\mu\mu}(\mu)} \qquad (3)$$

where $\nu = \nu_0 |\mu|^{q-1}$, $k_{\mathrm{res}} = \Omega/(\Gamma_p \mu v)$

Singularity at $\mu = \cos\alpha = 0$: **Cannot scatter through perpendicular point in phase space!**

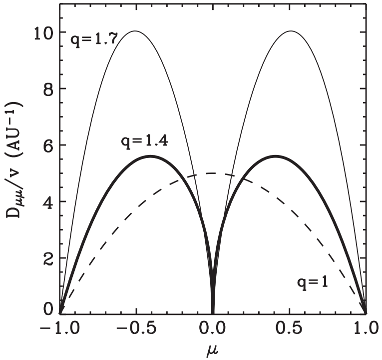

(e.g. Agueda & Vainio, 2013)

Problems with QLT

One way out:

- Allow "resonance broadening" from $\delta(k - \Omega/\Gamma_p \mu v)$ to more general but parametrized $\Gamma(k)$ (see also Dröge, 2000, 2003)

$\Rightarrow$ "Effective" resonant wavenumber $k_{\rm res} \sim \frac{\Omega}{\sqrt{(\mu\Gamma_p v)^2 + \delta^2 V_A^2}}$

Can fix the singularity, but there are more problems...

- "Wrong" diffusive behaviour for perpendicular transport (Shalchi et al., 2004)
- "Geometry" problem for parallel diffusion in non-slab models

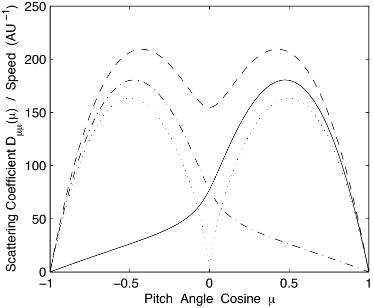

Beyond QLT

- Non-linear guiding centre theory (NLGC), Matthaeus et al. (2003): Solves 90° problem and perpendicular transport
- Weakly non-linear theory (WNLT)
- Second order QLT, Shalchi (2005): Correct orbits with result from QLT and re-substitute

Uses assumptions on higher-order correlations, theory becomes increasingly intractable...

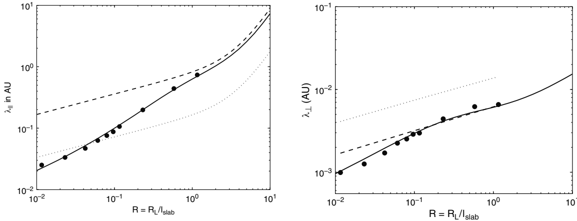

Parallel and perpendicular MFP in WNLT (solid), QLT (dashed), slab-QLT (dotted) and test-particle simulations (dots). Plotted against Larmor radius in units of correlation length.

For more, see the book "Nonlinear Cosmic Ray Diffusion" by Shalchi (2009).

Test particle transport simulations

- MHD simulation of e.g. driven turbulence
- "Push" particles, given the Lorentz force

$$\frac{d\mathbf{u}}{dt} = \frac{q}{mc}\left(\mathbf{E} + \frac{\mathbf{u}\times\mathbf{B}}{c\Gamma_{\mathrm{p}}}\right) + \mathbf{g} \tag{4}$$

can include radiation-reaction force $\mathbf{g}$. $\mathbf{E}, \mathbf{B}$ are the MHD electric and magnetic fields. Measure diffusion coefficients from particle positions:

$$D_{\mu\mu} = \lim_{t\to\infty}\frac{1}{2}\frac{\langle(\Delta\mu)^2\rangle}{t}\,; \qquad D_{pp} = \lim_{t\to\infty}\frac{1}{2}\frac{\langle(\Delta p)^2\rangle}{t} \tag{5}$$

Alternatively, use Taylor-Green-Kubo formulation

$$D_{\mu\mu} = \int_0^\infty dt\langle\dot{\mu}(t)\dot{\mu}(0)\rangle\,; \qquad D_{ij} = \int_0^\infty dt\langle\tilde{v}(t)\tilde{v}(0)\rangle\,, i = x, y \tag{6}$$

Coefficients given by two-time correlations, e.g. $\dot{\mu}$, or guiding-centre velocity $\tilde{v}$

Test particle transport simulations

For example Wisniewski et al. (2012) and Spanier & Wisniewski (2011).

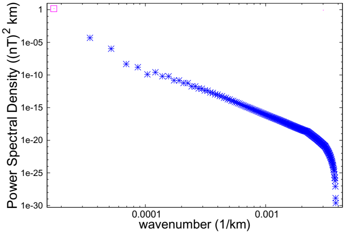

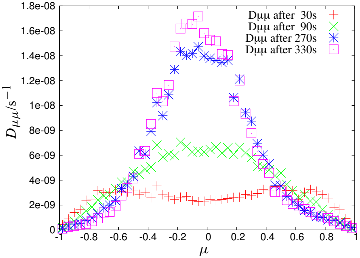

Use test-particle simulations to

- Check assumptions on non QLT theories
- Evaluate importance of non-resonant effects
- Include effect of δE, strong turbulence $\delta B/B > 1$
- Obtain "empirical" diffusion coefficients

Particle transport in Pulsar Wind Nebulae, Porth et al. (2013, 2014)

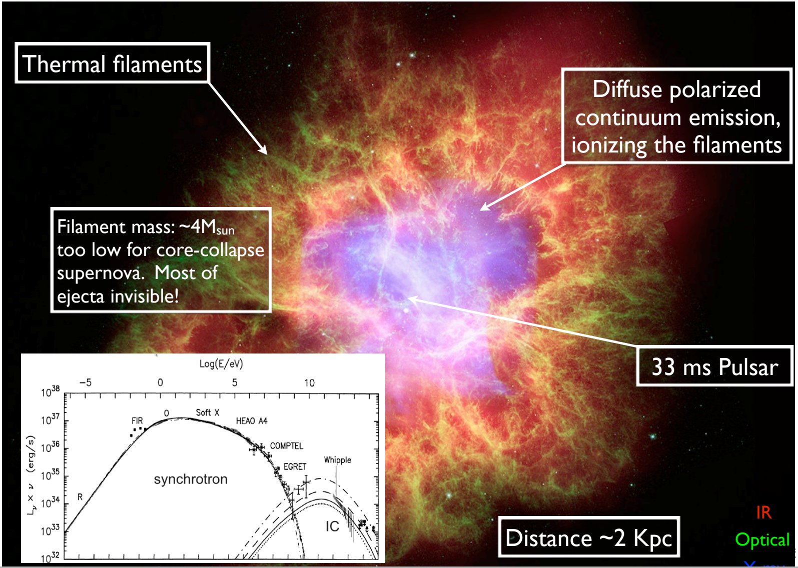

Particle transport in Pulsar Wind Nebulae

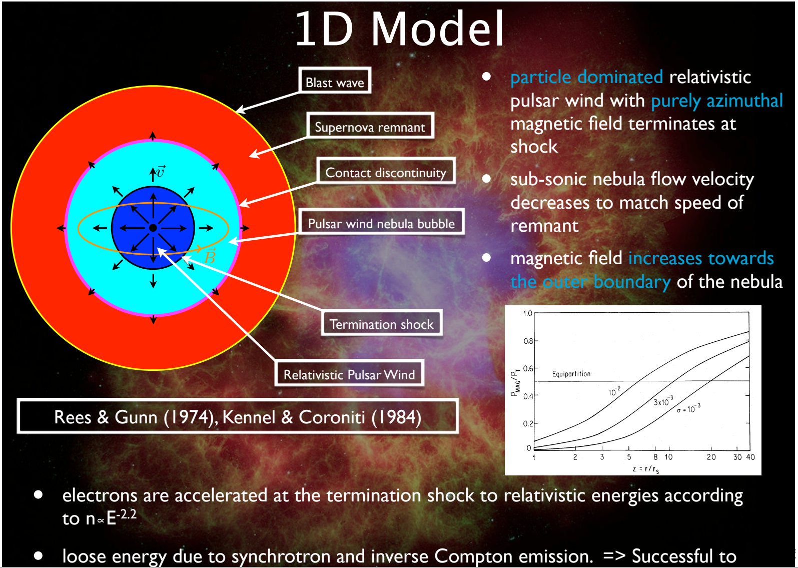

Covariant form of the equations

We can postulate the ideal MHD equations by demanding

Mass conservation

$$\nabla_\mu J^\mu = 0 \tag{7}$$

Energy and momentum conservation

$$\nabla_\mu T^{\mu\nu} = 0 \tag{8}$$

Maxwell's equations and ideal MHD

$$\nabla^*_\mu F^{\mu\nu} = 0,\ F^{\mu\nu} u_\nu = 0 \tag{9}$$

Equation of state

$$\epsilon = \epsilon(p, \rho) \tag{10}$$

∇_μ are covariant derivatives. These equations are valid in any frame (GR). For the PWN-application, we use Minkowski $\eta_{\mu\nu}$.

Particle transport in Pulsar Wind Nebulae

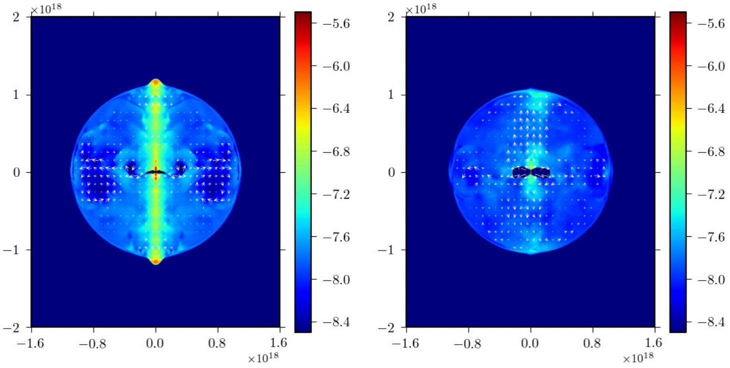

Particle transport in Pulsar Wind Nebulae

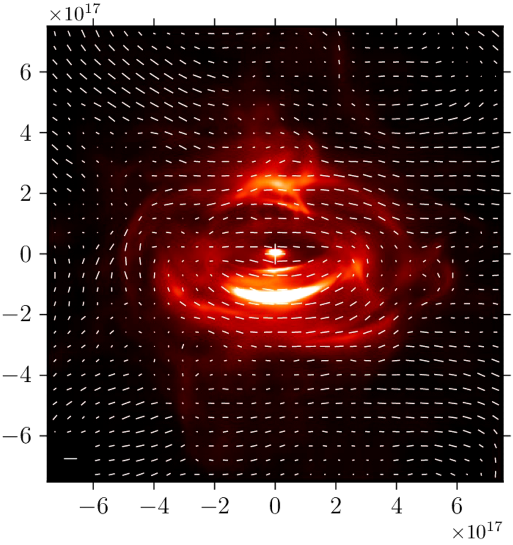

Particle transport in Pulsar Wind Nebulae

Magnetic field in the nebula

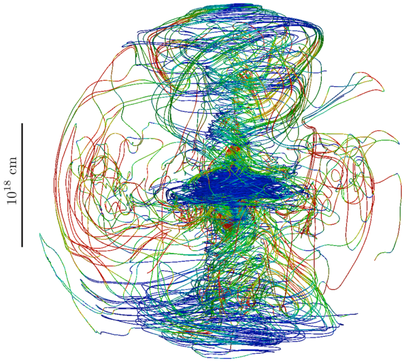

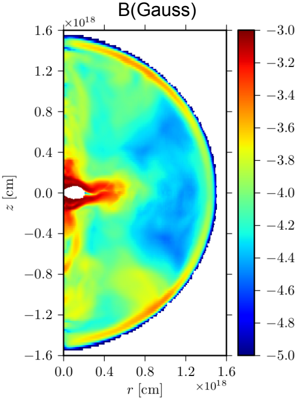

The magnetic field is strongest in the vicinity of the termination shock (in contrast to classical models), where it is still predominantly azimuthal. It is disordered further away from the shock.

Particle transport in Pulsar Wind Nebulae, **Work in progress with Michael Vorster, Eugene Engelbrecht and Maxim Lyutikov**

X-ray emitting leptons have Lorentz factors of $\Gamma_p \geq 10^7$

$$\frac{d\mathbf{u}}{dt} = \frac{q}{mc}\left(\mathbf{E} + \frac{\mathbf{u}\times\mathbf{B}}{c\Gamma_{\mathrm{p}}}\right) \tag{11}$$

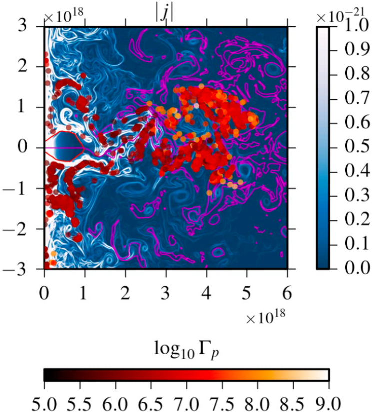

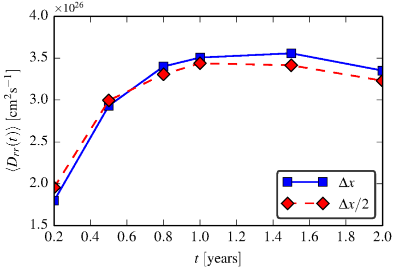

$$D_{rr}(t) = \frac{1}{2}\frac{\langle(\Delta r(t))^2\rangle_{r,\phi,\theta}}{t} \tag{12}$$

Particle transport in Pulsar Wind Nebulae

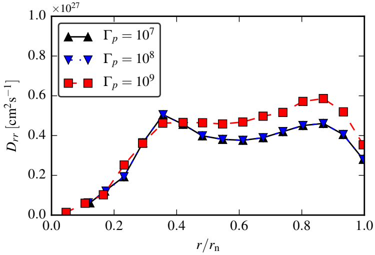

Average profile of the radial diffusion coefficient for increasing particle energies.

Bohm Diffusion:

$$D^{\mathrm{B}} = \frac{1}{3} r_g^2 \omega_g \tag{13}$$

$$= 1.7 \times 10^{26} \left(\frac{\Gamma_\mathrm{p}}{10^9}\right)\left(\frac{B}{100\mu\mathrm{G}}\right)^{-1} \mathrm{cm}^2\ \mathrm{s}^{-1} \tag{14}$$

Turbulent Eddy diffusion:

$$D^{\mathrm{E}}_{Ls} = \frac{1}{3} v_f L_\mathrm{s} \tag{15}$$

$$= 2.1 \times 10^{27} \left(\frac{v_f}{0.5c}\right)\left(\frac{L_\mathrm{s}}{0.42\mathrm{Ly}}\right) \mathrm{cm}^2\ \mathrm{s}^{-1}\,. \tag{16}$$

L_s : Scale of largest Eddy, termination shock $\sim 2 \times 10^{17}\,\mathrm{cm}$. v_f: Velocity at this scale $\sim 1/2c$.

$$r_g = \frac{p_\perp c}{eB} = 1.7 \times 10^{16} \left(\frac{\Gamma_\mathrm{p}}{10^9}\right)\left(\frac{B}{100\mu G}\right)^{-1} \mathrm{cm} \tag{17}$$

Diffusion becomes energy dependent when $r_g \geq L_s$, thus for $\Gamma_p = 10^{10}$, these particles have too short synchrotron lifetimes however $\Rightarrow$ Diffusion always energy independent!

Particle transport in Pulsar Wind Nebulae

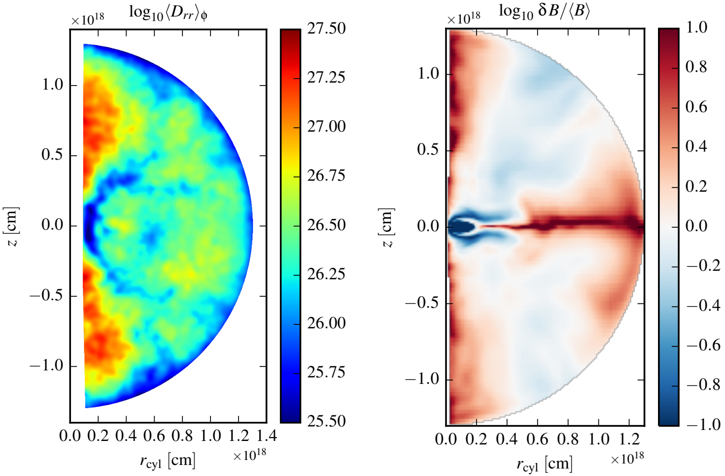

Map of the radial diffusion coefficient (left) and $\delta B/B$ measuring the strength of the turbulence. QLT would provide $D_{rr} \propto \delta B/B$

Particle transport in Pulsar Wind Nebulae

Back to the transport equation:

$$\frac{\partial f}{\partial t} + \mathbf{v} \cdot \nabla f = \frac{\partial}{\partial \mu}\left(D_{\mu\mu}\frac{\partial f}{\partial \mu}\right) + \frac{1}{p^2}\frac{\partial}{\partial p}\left(D_{pp}\frac{\partial f}{\partial p}\right) \tag{18}$$

Look for steady state solutions for the radial transport and including **adiabatic** and **radiative** losses:

$$D_{rr}(r)\frac{\partial^2 f}{\partial r^2}+\left[\frac{1}{r^2}\frac{\partial}{\partial r}\left(r^2 D_{rr}(r)\right) - V(r)\right]\frac{\partial f}{\partial r}+\left[\frac{1}{3r^2}\frac{\partial}{\partial r}\left(r^2 V(r)\right) + z_p p\right]\frac{\partial f}{\partial \ln p}+4z_p pf = 0, \tag{19}$$

with the Synchrotron loss term

$$z_p(r) = \frac{4\sigma_{\mathrm{T}}}{3\left(m_e c\right)^2}\frac{B^2(r)}{8\pi} \tag{20}$$

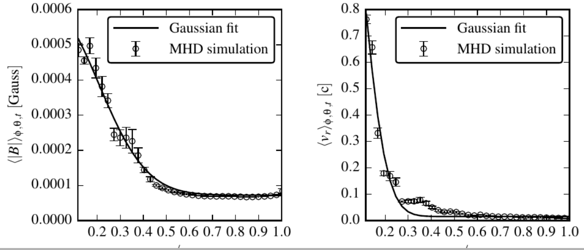

Particle transport in Pulsar Wind Nebulae: **Vela**

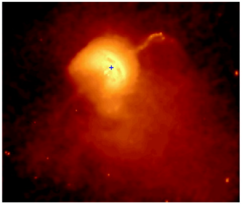

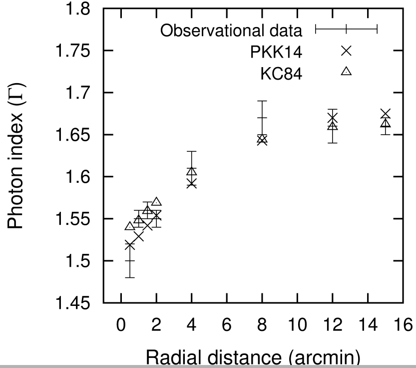

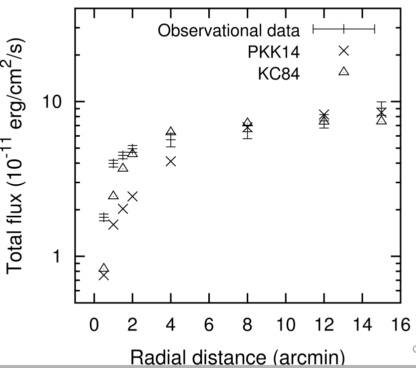

Particle transport in Pulsar Wind Nebulae: **G21.5-0.9**

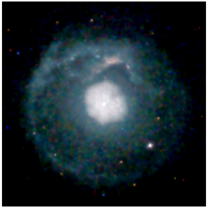

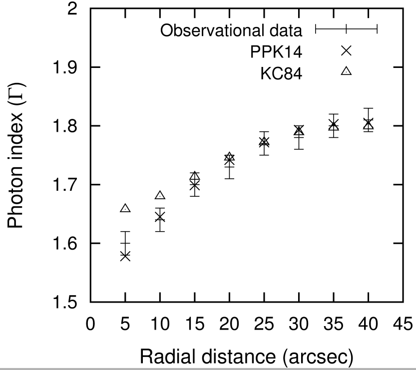

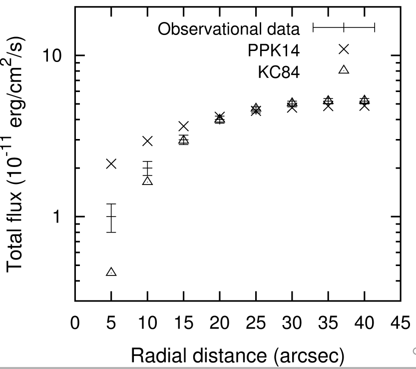

Particle transport in Pulsar Wind Nebulae: **3C58**

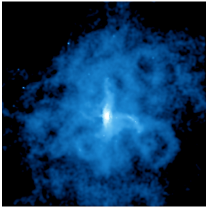

	G21.5-0.9		Vela		3C 58	
Parameter	KC84	PKK14	KC84	PKK14	KC84	PKK14
B_0 (μG)	11	283	24	38	2.2	300
V_0 (units of c)	0.36	0.51	0.43	0.51	0.35	0.51
κ_0 ($10^{26}\,\mathrm{cm^2\,s^{-1}}$)	55	5.7	1.6	1.4	12.1	13.3
σ (10^{-3})	1.3	$--$	55	$--$	0.55	$--$
η (10^{-2})	3.0	4.5	2.6	2.1	$--$	$--$
$\bar{B}$ (μG)	51	43	5.2	5.8	17	46
$\bar{V}$ (10^{-3}, units of c)	4.2	3.1	68	3.3	4.5	2.6
$\bar{\kappa}$ ($10^{26}\,\mathrm{cm^2\,s^{-1}}$)	11.5	5.7	8.1	1.4	1.7	13.3
$\bar{\xi}$	0.21	0.34	7.3	2.1	2.2	0.19

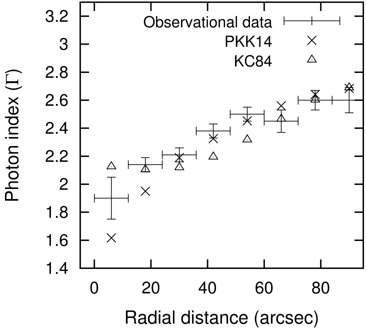

- Quality of fits based on re-scaled simulation models "as good/bad as" the laminar flow models
- Constrained parameters agree in order-of-magnitude with simpler analytic model
- Péclet number $\xi = \frac{Vr}{D_{rr}} = \mathcal{O}(1)$ thus diffusion important transport mechanism!

Model diffusive shock acceleration using SDE

Investigate diffusive shock acceleration

$$\frac{\partial f}{\partial t} = -(\boldsymbol{u}\cdot\nabla)f + \frac{1}{3}(\nabla\cdot\boldsymbol{u})p\frac{\partial f}{\partial p} + \nabla_i(D_{ij}\nabla_j f)$$
$$+ \frac{1}{p^2}\frac{\partial}{\partial p}\left(D_{pp}p^2\frac{\partial f}{\partial p} + a_{\rm syn}p^4 f\right),$$

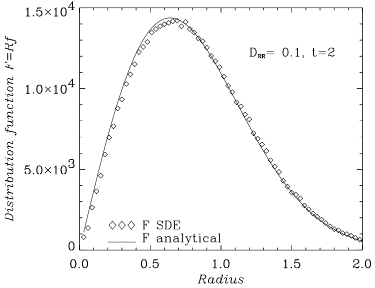

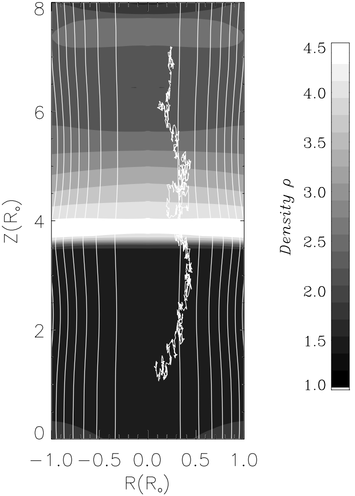

Casse & Marcowith (2003) Marcowith & Casse (2010)

The guiding centre approximation

- Direct Lorentz integration pointless when $R_L \equiv \frac{p_\perp c}{qB} \ll L$, with L being a typical scale of the MHD evolution.
- Decompose particle orbit

$$\mathbf{r} = \mathbf{R} + \boldsymbol{\rho} \tag{21}$$

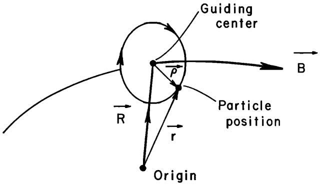

Fig. 1. The charged particle gyrates about its guiding center.

See textbook of Northrop (1963).

- Average over gyro-phase and derive equation of motion for the guiding centre **R**
- Decompose **R** into direction along the field line and across (drift)
- Decompose momenta into parallel $p_{||}$ and perpendicular $p_\perp$ components, $p_\perp^2/(2mB) = M = const$.

$$M = AI \tag{22}$$

$$A = \pi R_L^2;\; I = \frac{q\Gamma_p v_\perp / c}{2\pi R_L};\; R_L = \frac{p_\perp c}{qB} \Rightarrow M = \pi R_L^2 \frac{q\Gamma_p v_\perp}{2\pi R_L} = \frac{p_\perp^2}{2mB} \tag{23}$$

The guiding centre approximation, $E_{||}, E_{\perp} = \mathcal{O}(\epsilon)$

$$\frac{dR_{\perp}}{dt} = \frac{\mathbf{E}\times\mathbf{B}}{B^2} + \frac{\hat{b}}{B}\times\frac{p_{\perp}^2 c}{2B\Gamma_p qm}\nabla|B| + \frac{\hat{b}}{B}\times\frac{p_{||}^2 c}{\Gamma_p qm}(\hat{b}\cdot\boldsymbol{\nabla})\hat{b} \tag{24}$$

- "EcrossB" drift[1]

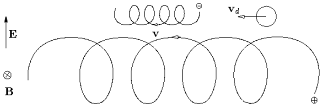

- "GradB" drift

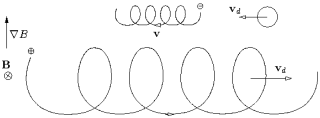

- "Curvature" drift

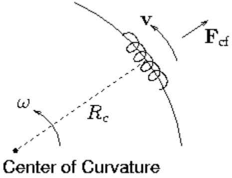

GC position:

$$\frac{d\mathbf{R}}{dt} = \frac{d\mathbf{R}_\perp}{dt} + \frac{p_{||}}{\Gamma_p m}\hat{\mathbf{b}} \tag{25}$$

Parallel momentum:

$$\frac{p_{||}}{dt} = qE_{||} - \frac{M}{\Gamma_p}(\hat{\mathbf{b}} \cdot \nabla)|\mathbf{B}| \tag{26}$$

- Direct acceleration
- "Mirror force"

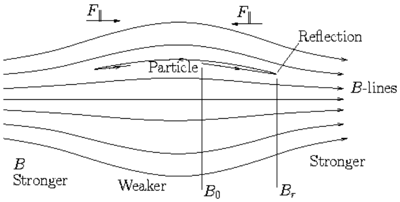

Perpendicular momentum:

$$\frac{p_\perp^2}{2Bm} \equiv M = const. \tag{27}$$

Applicability of the GCA, solar corona

Parameters for magnetic field magnitude B, temperature T, number density n, thermal speed $v_{thermal} = \sqrt{2k_B T/m_0}$, plasma beta $\beta = 2\mu n k_B T/B^2$, gyration radius $R_L = \gamma v_\perp m_0/qB$ and Lorentz factor γ respectively, for electrons and protons in the solar corona (Goedbloed & Poedts, 2004).

Typical values for plasma parameters in the solar corona

Particle	B $[T]$	T $[K]$	n $[m^{-3}]$	$v_{thermal}$ $[m/s]$	β $[-]$	R_L $[m]$	γ $[-]$
Electron	$0.03\ T$	$10^6\ K$	$10^{16}\ m^{-3}$	$5.5 \times 10^7\ ms^{-1}$	0.0004	$10^{-3}\ m$	1.0002
Proton	$0.03\ T$	$10^6\ K$	$10^{16}\ m^{-3}$	$1.3 \times 10^6\ ms^{-1}$	0.0004	$4.4 \times 10^{-2}\ m$	1.0000

Typical simulation $\mathcal{O}(10^6 m)$, resolution $\sim 300^3$: The orbiting motion takes place on approximately 10^{-8} of a grid cell (electrons) and on 5×10^{-7} of a grid cell (protons).

$\Rightarrow$ Gyrations completely unresolved! GCA well applicable.

Solar corona, example: Gordovskyy et al. (2014)

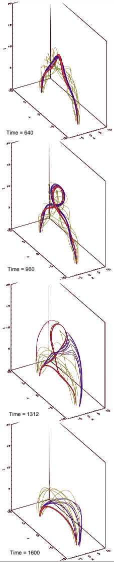

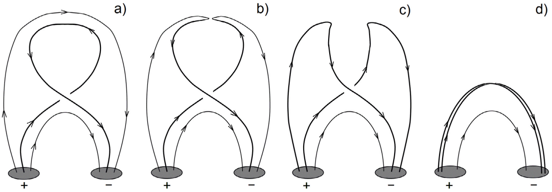

Twisted coronal loop, scale $2 \times 10^5\,\mathrm{m}$.

Follow GCA particles (+Coulomb collisions) in the kink-unstable MHD evolution.

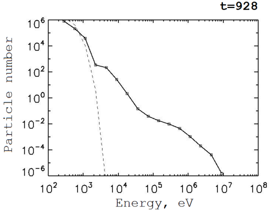

Electron spectra just after the onset of reconnection. Non-thermal tail thermalises slowly due to collisions.

Solar corona, example: Gordovskyy et al. (2014)

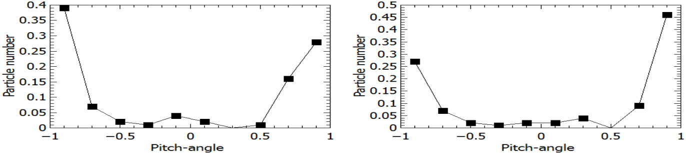

High energy pitch angle distribution during fast reconnection stage: Highly biased towards $|\mu| = 1$. Electrons (left) and protons (right).

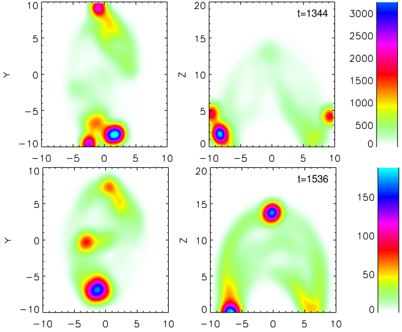

Synthetic Bremsstrahlung intensity at $10\,\mathrm{keV}$ based on test-particle distribution

$$I(\epsilon) \propto \int_{\epsilon}^{\infty} \int_{L} N(E, l) \frac{n(l)}{\epsilon\sqrt{E}} dE dl \qquad (28)$$

(Kontar et al., 2002)
Initially, emission concentrated at footpoints, moving up as time progresses. Higher density case more uniform emission.

Hands-on examples

Particle equations of motion implemented

- Advection
- Lorentz force
- relativistic GCA

Particle acceleration in the tilt-kink instability: Keppens et al. (2014)

The "tilt" is an ideal MHD instability of two repelling current channels (Richard et al., 1990)

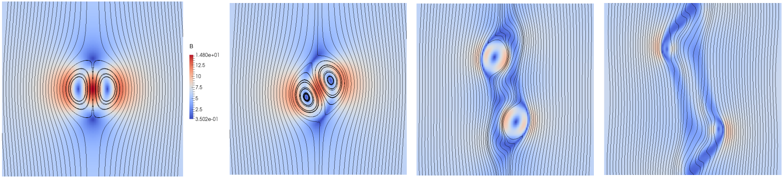

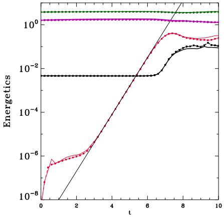

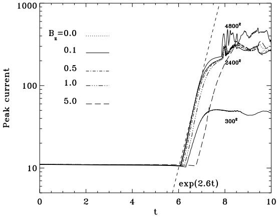

- Very fast (exponential) formation of current sheets
- 2D evolution near independent of guide-field

Particle acceleration in the tilt-kink instability: Keppens et al. (2014)

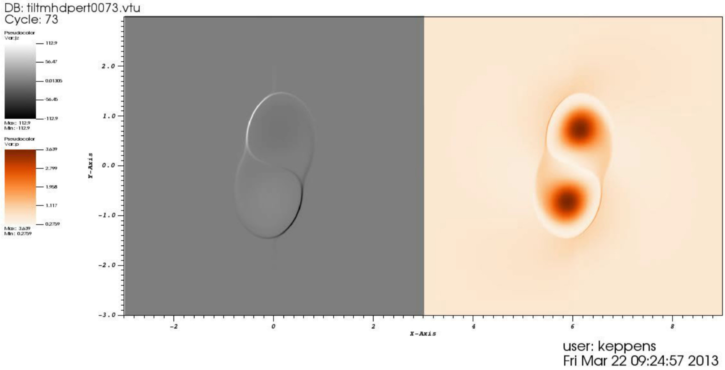

Particle acceleration in the tilt-kink instability: Keppens et al. (2014)

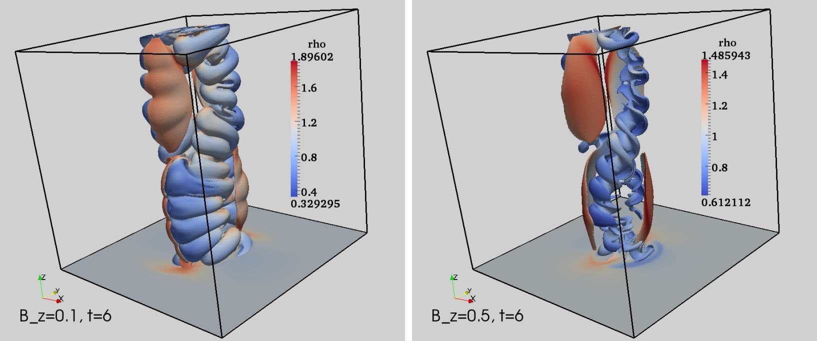

X-point collapse

Force-free electrodynamics

$$\partial_t \Phi + \boldsymbol{\nabla} \cdot \boldsymbol{B} = -\kappa \Phi$$

$$\partial_t \boldsymbol{B} + \boldsymbol{\nabla} \times \boldsymbol{E} + \nabla \Phi = 0$$

$$\partial_t \Psi + \boldsymbol{\nabla} \cdot \boldsymbol{E} = q - \kappa \Psi$$

$$\partial_t \boldsymbol{E} - \boldsymbol{\nabla} \times \boldsymbol{B} + \nabla \Psi = -\boldsymbol{J}$$

$$\partial_t q + \boldsymbol{\nabla} \cdot \boldsymbol{J} = 0$$

$$\boldsymbol{J} = q \boldsymbol{v_d} + \kappa_{||} \boldsymbol{E}_{||} + \kappa_{\perp} \boldsymbol{E}_{\perp}$$

$$\boldsymbol{v_d} = \frac{\boldsymbol{E} \times \boldsymbol{B}}{B^2}$$

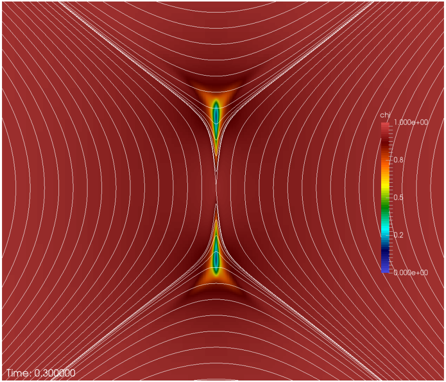

X-point collapse

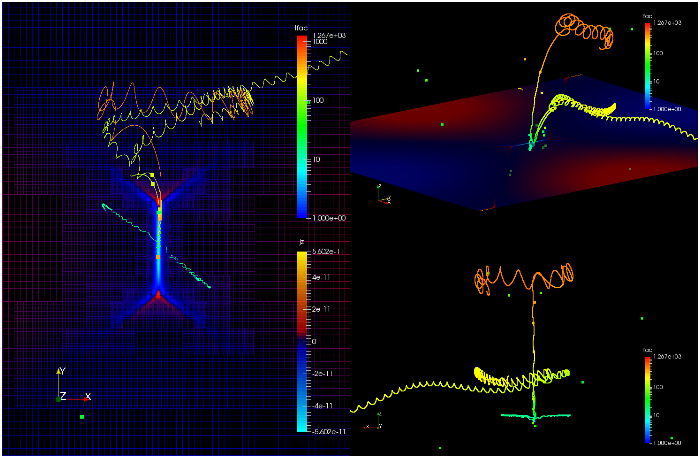

Coalescence Instability

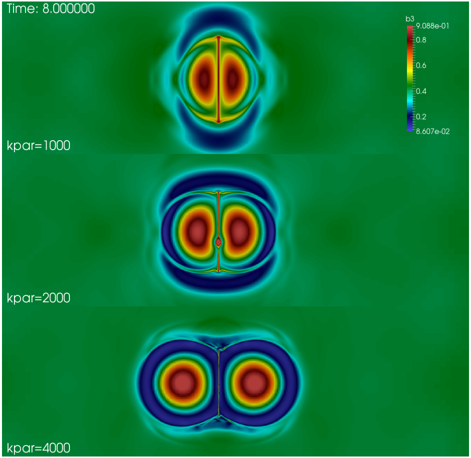

Coalescence Instability

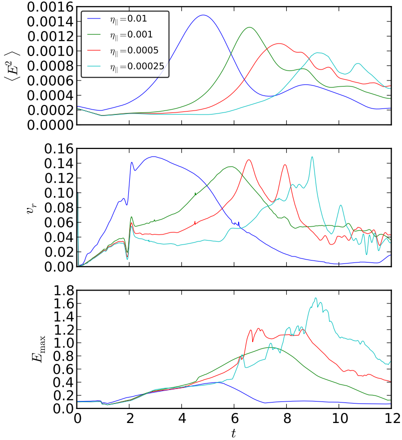

ParticleSnapshot

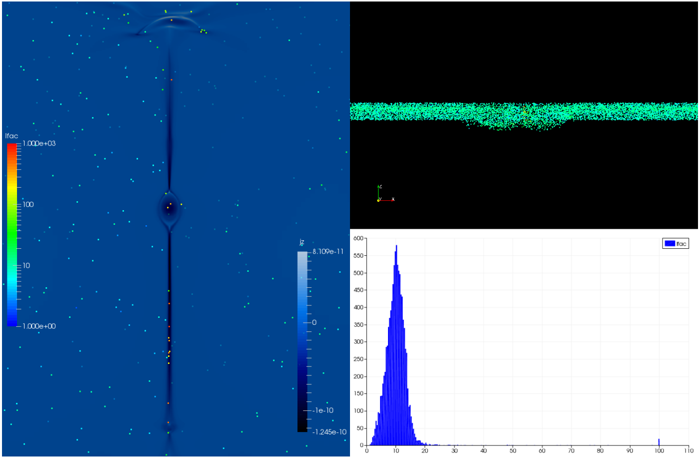

The relativistic guiding centre approximation

$$\frac{d\mathbf{R}}{dt} = \frac{(\gamma v_{\|})}{\gamma}\hat{\mathbf{b}} + \frac{\hat{\mathbf{b}}}{B\left(1-\frac{E_\perp^2}{B^2}\right)} \times \left\{ -\left(1-\frac{E_\perp^2}{B^2}\right) c\mathbf{E} + \frac{\mu_r c}{\gamma q}\nabla\left[B\left(1-\frac{E_\perp^2}{B^2}\right)^{1/2}\right]\right.$$
$$\left. + \frac{c m_0 \gamma}{q}\left(v_{\|}^2\left(\hat{\mathbf{b}}\cdot\nabla\right)\hat{\mathbf{b}} + v_{\|}\left(\mathbf{u_E}\cdot\nabla\right)\hat{\mathbf{b}} + v_{\|}\left(\hat{\mathbf{b}}\cdot\nabla\right)\mathbf{u_E} + \left(\mathbf{u_E}\cdot\nabla\right)\mathbf{u_E}\right) + \frac{v_{\|}E_{\|}}{c}\mathbf{u_E}\right\} + \mathcal{O}\left(\epsilon^2\right), \tag{29}$$

$$\frac{d\left(m_0\gamma v_{\|}\right)}{dt} = m_0\gamma\mathbf{u_E}\cdot\left(v_{\|}^2\left(\hat{\mathbf{b}}\cdot\nabla\right)\hat{\mathbf{b}} + v_{\|}\left(\mathbf{u_E}\cdot\nabla\right)\hat{\mathbf{b}}\right)$$
$$+ qE_{\|} - \frac{\mu_r}{\gamma}\hat{\mathbf{b}}\cdot\nabla\left[B\left(1-\frac{E_\perp^2}{B^2}\right)^{1/2}\right] + \mathcal{O}\left(\epsilon^2\right), \tag{30}$$

$$\frac{m_0\gamma^{*2}v_\perp^{*2}}{2B^*} = M = \text{constant}, \tag{31}$$

References

Agueda N., Vainio R., 2013, Journal of Space Weather and Space Climate, 3, A10

Casse F., Marcowith A., 2003, A&A, 404, 405

Dröge W., 2000, Space Sci. Rev., 93, 121

Dröge W., 2003, ApJ, 589, 1027

Goedbloed J. P. H., Poedts S., 2004, Principles of Magnetohydrodynamics

Gordovskyy M., Browning P. K., Kontar E. P., Bian N. H., 2014, A&A, 561, A72

Jackson A. A., 2001, Planet. Space Sci., 49, 417

Jokipii J. R., 1966, ApJ, 146, 480

Keppens R., Porth O., Xia C., 2014, ArXiv e-prints

Kontar E. P., Brown J. C., McArthur G. K., 2002, Sol. Phys., 210, 419

Kress B. T., Hudson M. K., Looper M. D., Albert J., Lyon J. G., Goodrich C. C., 2007, Journal of Geophysical Research (Space Physics), 112, 9215

Kress B. T., Hudson M. K., Looper M. D., Lyon J. G., Goodrich C. C., 2008, Journal of Atmospheric and Solar-Terrestrial Physics, 70, 1727

Marcowith A., Casse F., 2010, A&A, 515, A90+

Matthaeus W. H., Qin G., Bieber J. W., Zank G. P., 2003, ApJ, 590, L53

Northrop T. G., 1963, Reviews of Geophysics and Space Physics, 1, 283

Porth O., Komissarov S. S., Keppens R., 2013, MNRAS, 431, L48

Porth O., Komissarov S. S., Keppens R., 2014, MNRAS, 438, 278

Richard R. L., Sydora R. D., Ashour-Abdalla M., 1990, Physics of Fluids B, 2, 488

Shalchi A., 2005, Physics of Plasmas, 12, 052905

Shalchi A., ed. 2009, Nonlinear Cosmic Ray Diffusion Theories Vol. 362 of Astrophysics and Space Science Library

Shalchi A., Bieber J. W., Matthaeus W. H., Qin G., 2004, ApJ, 616, 617

Spanier F., Wisniewski M., 2011, Astrophysics and Space Sciences Transactions, 7, 21

Wisniewski M., Spanier F., Kissmann R., 2012, ApJ, 750, 150